ELSEVIER

Journal of Organometallic Chemistry 635 (2001) 92–99

Journal of Organometallic Chemistry

www.elsevier.com/locate/jorganchem

The relevance of the Dewar model to neighboring p-block element analogs of metal hydrocarbon π-complexes

Thomas P. Fehlner *

Department of Chemistry and Biochemistry, University of Notre Dame, Notre Dame, IN 46556, USA

Received 5 March 2001; accepted 16 April 2001

Abstract

The existence of p-block element analogs of transition metal hydrocarbon π-complexes presents opportunities to examine the appropriateness of the Dewar model in describing the metal–main group η^2-bonding interaction. Geometric structures and molecular orbital descriptions of electronic structures reveal both similarities and differences in the mutual perturbation of the metal and main group atom centers. Literature examples containing boron, silicon and phosphorus are used to illustrate the point in detail and the variety of metallaborane analogs of larger hydrocarbon π-complexes illustrates the scope of possibilities.

Keywords: Metallaboranes; Metallasilanes; Metallaphosphanes

1. Introduction

Unsaturated hydrocarbons constitute a significant fraction of organic compounds and our understanding of their interaction with metal centers depends heavily on the simple, but effective, Dewar–Chatt–Duncanson (DCD) model [1,2]. The chemistry associated with metal–polyene complexes also constitutes a large fraction of the modern interdisciplinary field known as organometallic chemistry [3]. Growing slowly but steadily is an analogous chemistry based on the complex interaction of metals with the other p-block elements surrounding carbon in the periodic table. Some of these compounds are, in fact, isoelectronic with metal–hydrocarbyl complexes of various types and their structural and reaction chemistry has been incorporated into a cross-disciplinary field analogous to organometallic chemistry which has been called inorganometallic chemistry [4]. A subset, similar to metal–polyene complexes, provides an opportunity to explore the applicability of the DCD model outside of carbon-based chemistry. The compounds discussed below demonstrate the usefulness of the model in areas almost certainly not considered by its originators 50 years ago.

2. The Dewar–Chatt–Duncanson model

The relevant essentials of the DCD model for metal–olefin coordination are summarized in Fig. 1 [5]. In this qualitative molecular orbital (MO) description, it is seen that the overall bond between the metal center and hydrocarbon arises from two major interactions. Both are Lewis acid–base interactions. That designated (a) of σ-symmetry with respect to the metal-C_2 centroid axis is no different from the one used to describe the primary metal–ligand bond between an electropositive metal center and an electron-rich ligand albeit the side-on binding was unusual at the time it was described. The two partners exchange roles in the interaction designated (b), which is of π-symmetry relative to the same axis. The ligand acts as an acceptor utilizing a C–C antibonding orbital and the metal as an electron donor via filled d-orbitals. Although clearly associated

* Fax: +1-219-6316652.
E-mail address: fehlner.1@nd.edu (T.P. Fehlner).

0022-328X/01/$ - see front matter
PII: S0022-328X(01)00857-9

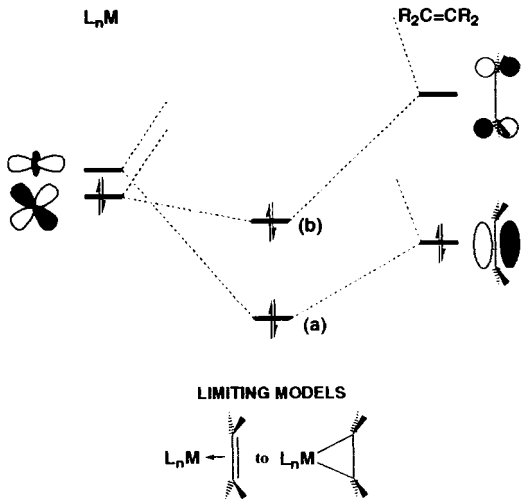

Fig. 1. Schematic representation of the σ ligand to metal and π metal to ligand donor–acceptor interactions in the DCD model.

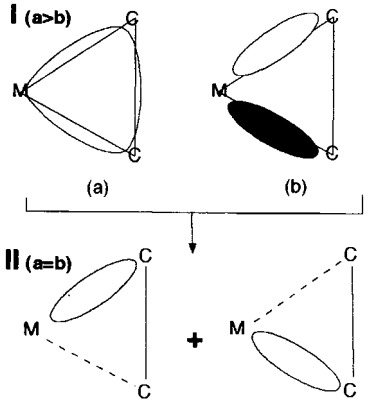

Fig. 2. Representations of the molecular orbitals associated with the σ ligand to metal and π metal to ligand donor–acceptor interactions in the DCD model in the two limiting cases **I** and **II**.

with Pauling's electroneutrality principle when applied to η^1-ligands in metal complexes, e.g. metal carbonyls, its application to multicentered, carbon-based (polyhapto) ligands provided an explanation of the geometric perturbation of the olefin on binding as well as conformational preferences and rotational barriers [5]. This review addresses the applicability of the two-part DCD model to the coordination of other multicenter, p-block element ligands to transition metal fragments.

The two components of the overall metal–ligand bond generates two limiting cases. In the first, **I**, the backbonding interaction (b) is small and (a) alone describes the bonding interaction. In this case, the donor–acceptor bond is largely a three-center σ-bond not unlike the three-center B–B–B bond utilized by Lipscomb in his localized model for the polyhedral boranes (Fig. 2a) [6]. In the second limiting case, **II**, the two interactions are approximately equal and transform into a pair of localized metal–carbon single bonds (metallacyclopropane). In the first limiting case, more of the electron density corresponding to the bond is expected to lie within the triangle defined by the metal and two carbon atoms than in the second case. Likewise, the pyramidalization at carbon will increase in going from the first to the second case and the two interactions are seen to represent two of the three Walsh orbitals of cyclopropane [7]. The third is largely C–C bonding. Although the original DCD model was based on a perturbation theory approach, there is a smooth, qualitative correlation between the limits. Indeed, known complexes lie somewhere in between and the model serves to connect structure with properties of the transition metal and its ancillary ligands as well as with the substituents on the olefin [5]. It is the purpose of this review to introduce another possible variable — the identity of the two p-block elements bound to the metal center. If one goes from carbon to boron to silicon to phosphorus, how does the variation in p-block element properties change the nature of the overall metal–ligand interaction?

3. Main group analogs of metal–olefin complexes

3.1. Boranes

Boron analogs of mononuclear ethylene metal complexes have been synthesized in the laboratories of Shore [8]. As illustrated in Eq. (1), these Group 8 metal complexes are assembled from monoboranes. Of particular interest is the neutral analog:

$$[M(CO)_4]^{2-} + 3BH_3THF \rightarrow [(CO)_4M)(\eta^2\text{-}B_2H_5)]^- + [BH_4]^-; \quad M = Fe, Ru, Os \tag{1}$$

$CpFe(CO)_2(\eta^2\text{-}B_2H_5)$, $Cp = \eta^5\text{-}C_5H_5$, which has been the focus of a valence level photoelectron spectroscopic study [9]. The metal–borane geometry is similar in all these compounds and is represented schematically in Fig. 3a. The orientation of the B_2H_4 moiety with respect to the metal center is qualitatively similar to that of C_2H_4 in a metal complex. The extra BHB bridging hydrogen lies in the MB_2 plane, i.e. the metal fragment effectively replaces a bridging hydrogen atom in diborane.

Hence, it is appropriate to first examine the perturbation of the frontier orbitals of a planar B_2H_4 fragment by two hydrogen atoms to generate diborane. This is illustrated in Fig. 4 where it may be seen that the symmetric and antisymmetric combinations of the H 1s orbitals stabilize the B–B σ- and B–B π-bonding orbitals, respectively. This is a large effect as shown in the classic paper comparing the photoelectron spectra of B_2H_6 and C_2H_4 [10]. For symmetry reasons the π*-MO of B_2H_4 is unaffected and, in the absence of pyramidal-

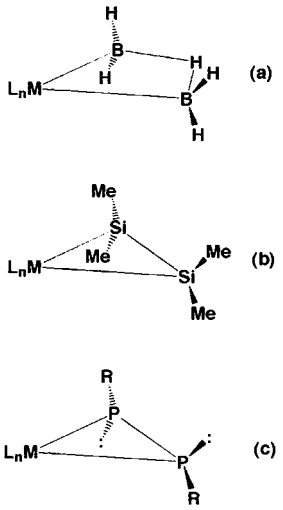

Fig. 3. The known geometric structures of: (a) boron; (b) silicon; and (c) phosphorus analogs of a $L_nM(\eta^2\text{-}C_2H_4)$ complex.

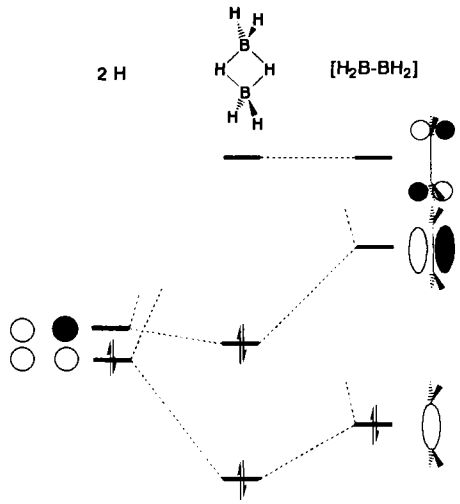

Fig. 4. Schematic representation of the perturbation of an ethylenic B_2H_4 fragment by two bridging hydrogen atoms to generate diborane (6).

ization at boron, remains at high energy with consequences described below.

A first order description of the metal complex is generated by simply replacing one bridging hydrogen atom with either the $[M(CO)_4]^-$ or $CpFe(CO)_2$ one electron metal fragment. Based on the relevant ionization energies, the three center, two electron bonding MO of the metallaborane, corresponding to interaction (a) in Figs. 1 and 2, lies lower in energy than that of $(CO)_4Fe(\eta^2\text{-}C_2H_4)$ (-11.4 vs. -10.6 eV) but higher in energy than the π-MO of diborane (-11.4 vs. -14.7 eV). This is consistent with the fact that one bridging proton remains and with the softer metal center versus hydrogen. Fenske–Hall calculations show that this principal metal–main group element bonding MO has large metal and main group contents for both B_2H_5 and C_2H_4 moieties. Thus, the metal–ligand interaction (a) in Figs. 1 and 2 is similar in both compounds.

There is, however, a significant difference between interaction (b), Figs. 1 and 2 in the boron and carbon derivatives. The high energy of the B_2H_4 orbital which corresponds to the π^*-orbital of C_2H_4 (see above) leads to a weaker interaction with the filled d orbitals on the metal center. Thus, the B_2H_5 contribution to interaction (b) is smaller than found for the ethylene complex. In the DCD model, the perturbation of the primary ligand to metal donor acceptor interaction is distinctly less for the borane relative to the hydrocarbon. This conclusion is consistent with the geometric parameters: the B–B distance (Table 1) is nearly the same as in B_2H_6 and the B_2H_4 ethylenic fragment is nearly planar.

Note also that the B–B distance is substantially longer than the C–C distance in the metal complexes being compared (Table 1). Likewise, it is long compared to a diborane exhibiting a double bond, $Li_2[B_2R_4]$ [11]. Hence, the 'extra' hydrogen atom found bridging the two boron atoms cannot be considered an innocent spectator as far as the metal–boron interaction is concerned. The bridging hydrogen creates the effect of pyramidalization at boron for the ligand donor interaction (a). However, as the B_2H_4 fragment is still planar, the π^*-acceptor orbital remains at high energy. Consequently, the structural response of olefins on η^2-coordination that lowers the energy of the ligand acceptor

Table 1
Change in E–E distance on η^2-coordination

E_2R_4	d_{E-E} (Å)	$d_{E=E}$ (Å)	$L_nM(\eta^2\text{-}E_2R_2)$			References
			d_{E-E} (Å)	L_nM	R	
C	1.56	1.33	1.46	$(CO)_4Fe$–	H	[3]
B	1.77 [a], 1.86 [b]	1.64 [b]	1.80 [c]	$(CO)_4Fe$–	H	[8,9,11]
Si	2.35	2.14	2.26	Cp_2W–	Me	[13]
P	2.20	2.03	2.14	Cp_2Mo–	H	[19]

[a] B_2H_6.
[b] $[B_2R_4]^{2-}$.
[c] $[B_2H_5]$.

orbital and enhances the backbonding interaction is unavailable for the borane. An isoprotonic borane analog of $(CO)_4Fe(\eta^2\text{-}C_2H_4)$ might well show a closer relationship to an ethylene complex; however, a compound such as $[CpFe(CO)_2(\eta^2\text{-}B_2H_4)]^-$ is yet to be synthesized.

Although not isoelectronic with C_2H_4, the recent chemistry of diboryl metal complexes with both intact B_2R_4 and two separate BR_2 ligands provides a relevant extension of the above chemistry that is of considerable importance in understanding metal catalyzed boronation reactions [12]. This area has been recently reviewed [13].

3.2. Silanes

One expects a close similarity between an ethylene and a disilene–metal complex as both carbon and silicon are Group 14 elements. Still, silicon with its diagonal relationship to boron provides an interesting test of the generality of the DCD model. It was not until a decade ago that synthetic routes to these species were successfully worked out in spite of the fact that disilenes had been isolated 10 years earlier. However, the characterization of free disilenes depends upon the use of sterically demanding substituents to prevent polymerization — a factor which also inhibits coordination to a metal center. Hence, indirect routes were devised to produce the desired compounds. These are illustrated for Group 10 and 6 metals in Eqs. (2) and (3), respectively [14,15]. Both are based on metallacycle ring closure in a metal bound η^1-disilane containing a direct M–Si bond.

$$\begin{aligned}
&dppePt(\eta^2\text{-}C_2H_4) + (R_2SiH)_2 \rightarrow dppePt(H)(SiR_2SiR_2H)\\
&dppePt(H)(SiR_2SiR_2H)_2 \rightarrow dppePt(\eta^2\text{-}Si_2R_4)
\end{aligned} \tag{2}$$

$$\begin{aligned}
&Li[Cp_2WH] + ClSiMe_2SiMe_2Cl\\
&\quad \rightarrow Cp_2W(H)SiMe_2SiMe_2Cl\\
&Cp_2W(H)SiMe_2SiMe_2Cl + CCl_4\\
&\quad \rightarrow Cp_2W(Cl)SiMe_2SiMe_2Cl\\
&Cp_2W(Cl)SiMe_2SiMe_2Cl + Mg \rightarrow Cp_2W(\eta^2\text{-}Si_2Me_4)
\end{aligned} \tag{3}$$

This brief discussion is focused on the tungsten derivative as a solid state structure is available [15]. As illustrated in Fig. 3b, $Cp_2W(\eta^2\text{-}Si_2Me_4)$ constitutes a straightforward geometric analog of an ethylene–metal complex — there are no extra atoms to confuse the connection. The Si–Si bond distance falls midway between the expected values for single and double bonds thereby suggesting that interaction (b), Fig. 2, constitutes a significant part of the overall metal–silicon bonding (Table 1). Consistent with this conclusion, the pyramidalization at silicon lies between that expected for sp^2 and sp^3 hybridized silicon atoms. It is, however, somewhat less that observed for carbon in complexes with low-valent early transition metals, e.g. $Cp^*_2Ti(\eta^2\text{-}C_2H_4)$, $Cp^* = \eta^5\text{-}C_5Me_5$ [16]. Unquestionably, $Cp_2W(\eta^2\text{-}Si_2Me_4)$ constitutes both a structural and electronic analog of a metal–ethylene complex well described by the DCD paradigm.

This conclusion is reinforced by calculational studies which permit the overall interaction to be dissected into its component parts [17,18]. Relative to a d^{10} ML_2 fragment the disilene is found to be more strongly bound than C_2H_4. The work suggests that the disilene complex is best described with a metallacyclopropane limiting structure suggesting interactions (a) and (b), Figs. 1 and 2, of comparable strengths. Like borane, but in contrast to C_2H_4, the electronegativity of silicon is close to that of a transition metal leading to a better match between the energies of the π-donor orbital and the metal acceptor orbital. Previously, we suggested that, in a comparison of metallaboranes with analogous hydrocarbyl complexes, stronger metal–main group binding is associated with a better match of metal and main group atom electronegativities [19]. In addition, unlike the borane and like C_2H_4, there is no bridging hydrogen and pyramidalization of the SiH_2 group permits the π*-acceptor orbital to better match the metal donor orbital. Both foster tighter binding to the metal center.

3.3. Phosphanes

Phosphorus enjoys a diagonal relationship with carbon and possesses an additional valence electron. Like disilenes, isolation of free diphosphene required the utilization of bulky substituents and consequently access to coordinated $\eta^2\text{-}P_2R_2$ required indirect approaches [20]. Two are illustrated in Eqs. (4) and (5); however, several others have been successfully employed [21].

$$Cp_2WH_2 + P_4 \rightarrow Cp_2W(\eta^2\text{-}P_2H_2) \tag{4}$$

$$dppePtCl_2 + Li_2[P_2R_2] \rightarrow dppePt(\eta^2\text{-}P_2R_2) \tag{5}$$

As illustrated in Fig. 3c, a coordinated η^2-diphosphene adopts a *trans* conformation and the lone pair on each phosphorus atom occupies the position of one R group in the analogous disilene compound. The P–P bond distance in these compounds also falls between the values of P–P single and double bonds (Table 1). Although a single number cannot be used to define the extent of interaction (b) versus (a) in Figs. 1 and 2, the similarities of the geometric changes on coordination for carbon, silicon and phosphorus suggest the DCD model is appropriately applied to phosphorus as well.

The lone pairs on a diphosphene constitute Lewis basic sites that compete with the double bond for the

Table 2
Chemical shift changes on η^2-coordination

E=E	Nucleus	$\Delta\delta$ (ppm)
C	^{13}C	−80
B	^{11}B	−30 [a], −110 [b]
Si	^{29}Si	−420
P	^{31}P	−370

$\Delta\delta = \delta(E{=}E)_{bound} - \delta(E{=}E)_{free}$.
[a] vs. B_2H_6.
[b] vs. $[B_2R_4]^{2-}$.

acidic metal site. Indeed a substantial number of η^1-complexes as well as mixed complexes are known [21]. In these, the P–P bond length retains the value corresponding to a double bond as found in free diphosphenes. The mixed complexes provide a rough internal measure of the overall strength of the two different metal–ligand interactions. Thus, for example, $(CO)_5Cr\{\eta^2\text{-}P_2(\eta^1\text{-}Cr(CO)_5)_2Ph_2\}$ generates free $P_2(\eta^1\text{-}Cr(CO)_5)_2Ph_2$ on heating suggesting that the double bond coordinates less strongly than a lone pair [22]. However, as η^1-coordination of P_2H_2 to a metal center is not a simple Lewis acid–base interaction, this observation is difficult to quantify [23].

Indeed a calculational study suggests that the η^2-binding mode is energetically favored over η^1-coordination by 25 kcal mol^{-1} for a d^{10} ML_2 metal fragment [24]. The origin of the preference for the η^2-structure results from maximum π-backbonding, interaction (b), Fig. 1. Assuming the same preference for a d^6 ML_5 fragment, the experimental results above reflect differences in kinetic barriers to dissociation, i.e. a larger barrier for η^1- versus η^2-dissociation. In turn, a larger barrier for a simple acid–base association than for η^2-coordination would be required. As this seems unlikely, the relative strength of the two binding modes must depend on the metal.

3.4. NMR shift changes on coordination

The E_2 fragments, E = C, B, Si, P, of all of these complexes have readily observable NMR active nuclei thereby providing another means of examining the metal–ligand interaction. Although the connection between chemical shift and electronic structure is far from transparent [25], a large shift to higher field empirically characterizes the ^{13}C signals of olefinic carbon atoms on η^2-coordination to a metal center [3]. As shown in Table 2, the same is true of the main group analogs of silicon and phosphorus. As a chemical shift for the free borane ligand, $[B_2H_5]^-$, is unavailable, the shift change on coordination can only be estimated using either $[B_2R_4]^{2-}$ or B_2H_6 as reference. The limits thereby placed on $\Delta\delta$ show that the coordinated borane also possesses more highly shielded boron atoms. As $\Delta\delta$ ultimately arises from the change in the electron distribution surrounding the main group atom E, the qualitative similarity in the shift change argues for similarity in the η^2-ligand to metal binding.

One can be more specific, albeit in an over simplified approach. In the Ramsey model large changes in shielding are associated with filled and unfilled MOs lying near the HOMO–LUMO gap which possess high p character of the NMR active element (the so-called paramagnetic term) [25]. Major contributors to this term in the free, doubly bonded E_2R_2, E = C, B, Si, P, ligand will arise from the p character of filled E–E and E–R σ bonding MOs combined with the unfilled E–E π*-antibonding MO as well as the filled E–E π-bonding MO with unfilled E–E and E–R σ antibonding MOs. In the DCD model, formation of the η^2-complex leads to destabilization of the empty π* and stabilization of the filled π-MO. Both changes lead to a decrease in the paramagnetic term and an increase in shielding. The large values of $\Delta\delta$ for Si and P reflect qualitatively similar changes in electronic structure on coordination. Even in the case of boron, the fact that $\Delta\delta$ is −30 ppm when B_2H_6 is used as reference shows that the metal is not simply acting as a proton. For $Cp(CO)_2Fe(\eta^2B_2H_5)$ and $[(CO)_4Fe(\eta^2B_2H_5)]^-$ the approximate calculations show that there is a significant interaction of filled metal based orbitals with the empty π*-MO (see above). This is reflected in the upfield shift on coordination consistent with application of the DCD model to the metal–ligand interaction. Presumably an even larger shift would be observed if the bridging hydrogen were removed from $Cp(CO)_2Fe(\eta^2B_2H_5)$ or a complex of $[B_2R_4]^{2-}$ were examined.

4. Metallaborane analogs of polyene–metal complexes

The DCD model finds extensions in the coordination of linear and cyclic polyolefins. Given the similarities between ethylene coordination and coordination of its neighboring inorganic analogs, one expects to observe analogs of coordinated polyolefins for the same elements. This is well illustrated for boron. Metallaboranes containing three and four boron atoms show that the existence of analogs of hydrocarbyl complexes in which the ligand acts as a π-acceptor is not restricted to the E_2 compounds discussed thus far [26–30].

4.1. Allyl complexes

One of the earliest metallaboranes characterized is $(R_3P)_2MB_3H_7$, M = Ni, Pd, Pt [31]. Since that time other examples containing Group 9 and 10 metals have been described: Ir [32,33], Pd [34,35] and Pt [36,37]. The routes are based on the coordination of a stable triborane as illustrated in Eq. (7).

$$[B_3H_8]^- + (R_3P)_2PtCl_2 + \text{base} \rightarrow (R_3P)_2Pt(\eta^3\text{-}B_3H_7) \quad (7)$$

$$[Cp^*IrCl_2]_2 + [BH_4]^- \rightarrow Cp^*IrH_2B_3H_7 + Cp^*IrH_4 \quad (8)$$

Recently routes to $Cp^*Co(CO)B_3H_7$ [38], $Cp^*Ru(CO)(H)B_3H_7$ [39], $Cp^*Ir(CO)B_3H_7$ and $Cp^*IrH_2B_3H_7$ [40] have been developed by building up the B_3 fragment from monoboranes, e.g. Eq. (8). $Cp^*Co(CO)B_3H_7$ is isoelectronic with $[CpCo(CO)(C_3H_5)]^+$ and the structures are compared in Fig. 5a. The relationship between the coordinated C_3H_5 and B_3H_7 moieties is analogous to that between coordinated C_2H_4 and B_2H_5 discussed above. That is, a proton is imbedded in each lobe of the three-center allyl π-bonding interaction forming BHB bridges that are *trans* to the metal center. As discussed previously [9], the effects of the bridges are also similar to those in $[(CO)_4Fe(\eta^2B_2H_5)]^-$ in that the B–B distances are larger than the C–C distances and the major metal–boron bonding occurs via a multi-center covalent interaction. The metal donor–triborane acceptor interaction is less than that in the η^3-allyl complex.

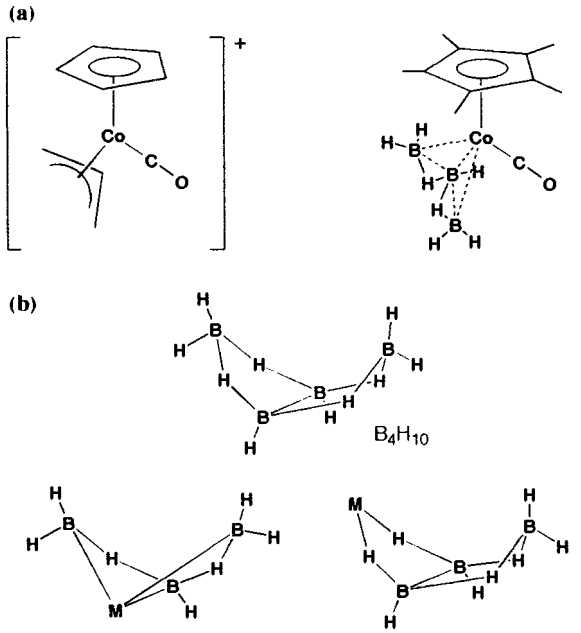

Fig. 5. (a) Comparison of the geometric structures of $[Cp(CO)Co(\eta^3\text{-}C_3H_5)]^+$ and its boron analog $Cp^*(CO)Co(\eta^3\text{-}B_3H_7)$. (b) The relationship of the geometric structure of $Cp^*(CO)Co(\eta^3\text{-}B_3H_7)$ with that of B_4H_{10} on the one hand and $(CO)_4MnB_3H_8$ on the other.

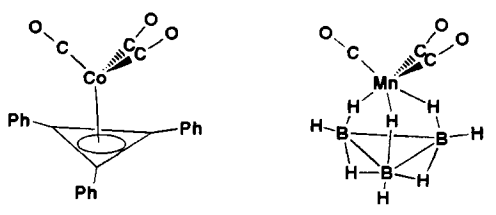

Fig. 6. Comparison of the geometric structure of $(CO)_3Co(\eta^3\text{-}C_3Ph_3)$ with that of $(CO)_3MnB_3H_8$.

The difference between the metallaborane and its organometallic analog is also expressed in a greater structural diversity which can be appreciated by comparison of the metal complex with its borane analog. Thus, as shown in Fig. 5b, $Cp^*Co(CO)B_3H_7$ is also an analog of B_4H_{10} in which the Cp*Co(CO) fragment replaces one of the two different borane fragments (BH and two bridging hydrogens). The other structural possibility, in which the metal fragment replaces a BH_2 group of B_4H_{10}, is well known and is also generated from the reaction of $[B_3H_8]^-$ with metal fragments containing halides [41,42]. We have intercompared the metal–ligand versus cluster representations of metallaboranes elsewhere [43].

4.2. Cyclopropyl complexes

Cyclopropenyl metal complexes are relatively small in number and there is only a single example of a metallaborane analog. It is formed by decarbonylation of a metallatriborane as shown in Eq. (9) [42]. Its structure is shown schematically

$$(CO)_4MnB_3H_8 \rightarrow (CO)_3MnB_3H_8 + CO \quad (9)$$

in Fig. 6 where it is compared with that of a typical organometallic analog. Now the connection between the two is less straightforward. The earlier transition metal and the switch from carbon to boron demands five addition hydrogens and three bridges between metal and boron atoms leaving one B–B edge unbridged. As already indicated, the presence of bridging hydrogens causes a large perturbation in the nature of the bonding of the two atoms bridged and one does not expect a simple connection between the electronic structures of the two species. In this case comparison of $(CO)_3MnB_3H_8$ with analogous clusters (B_4H_8 of limited stability on the one hand and $(CO)_6Fe_2B_2H_6$ on the other) are more useful.

4.3. 1,3-Butadienyl complexes

A few borane analogs of diene complexes are known. Initially, examples were prepared in Shore's laboratory by reaction of tetraborane anions with appropriate metal complexes as shown in Eq. (10) [44]. Later, we showed that similar compounds

$$[B_4H_9]^- + (R_3P)_2(CO)IrCl \rightarrow (R_3P)_2(CO)Ir(\eta^4\text{-}B_4H_9) \quad (10)$$

$$Cp^*IrH_2B_3H_7 + BH_3THF \rightarrow Cp^*Ir(H)B_4H_9 + H_2 \quad (11)$$

could be produced by borane addition to triborane derivatives as shown in Eq. (11) [45]. Once again, for these late transition metal derivatives the structural

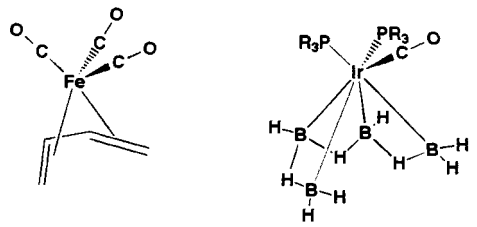

Fig. 7. Comparison of the geometric structure of $(CO)_3Co(\eta^4\text{-}C_4H_6)$ with that of $(PR_3)_2(CO)Ir(\eta^4\text{-}B_3H_9)$.

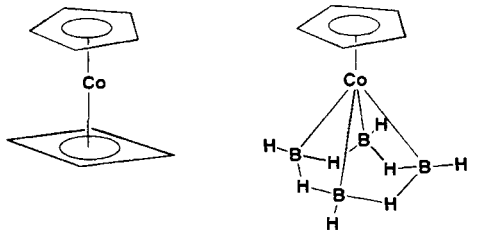

Fig. 8. Comparison of the geometric structure of $CpCo(\eta^4\text{-}C_4H_4)$ with that of $CpCo(\eta^4\text{-}B_4H_4)$.

analogy between organometallic and inorganometallic compounds is clear. As indicated in Fig. 7, a proton is embedded in each lobe of the four-center conjugated diene π-bonding interaction forming BHB bridges that are *trans* to the metal center. Indeed, the frontier orbitals of $[B_4H_9]^-$ largely mimic those of 1,3-butadiene [9].

4.4. Cyclobutadienyl complexes

Borane analogs of cyclobutadiene complexes were the ones that early on alerted chemists to the possibilities of a significant analog chemistry to that of polyhapto–polyene–metal complexes. The most thoroughly characterized is that of cobalt which is prepared as shown in Eq. (12). In this case, yields are low and the pathway is not clear [30,46–48]. The compound may also be isolated from the reaction of monoboranes with

$$CoCl_2 + [B_5H_8]^- + [Cp]^- \rightarrow CpCo(\eta\text{-}B_4H_8) \qquad (12)$$

monocyclopentadienyl cobalt halides; however, again the yield is very small [49]. Comparison of the structure with that of its organometallic analog (Fig. 8) once again reveals the same connection — four hydrogens bridge the B–B edges and lie on the face opposite to the metal atom.

5. Summary

Evidence has been presented for borane analogs of ferrocene [50] and there are related cyclo P_n, $n = 3$–6, metal complexes analogous to organometallic complexes with cyclic π-ligands [4]. However, complexes of $(SiR_2)_n$, $n > 2$, remain to be synthesized. A large difference between the inorganometallic and organometallic analogs is the extent to which the reaction chemistry has been investigated. Organometallic chemistry is well developed while the chemistry of the inorganometallic analogs is nearly unexplored. Consequently, the utility of the inorganometallic derivatives in manipulating main group or transition metal fragments is largely unknown. Partly this is a problem of accessibility but as synthetic routes are developed one expects the utility of these compounds to be more fully revealed. The intermediacy of mononuclear metallaboranes in successful approaches to the functionalization of hydrocarbons serves as a good reminder that new compound types add new tools to the chemist's workbox [51,52].

Acknowledgements

The support of the National Science Foundation is gratefully acknowledged.

References

[1] M.J.S. Dewar, Bull. Soc. Chim. Fr. 18 (1951) C71.
[2] J. Chatt, L.A. Duncanson, J. Chem. Soc. (1953) 2939.
[3] C. Elschenbroich, A. Salzer, Organometallics, VCH, New York, 1989.
[4] T.P. Fehlner (Ed.), Inorganometallic Chemistry, Plenum, New York, 1992.
[5] D.M.P. Mingos, in: E. Abel, F.G.A. Stone, G. Wilkinson (Eds.), Comprehensive Organometallic Chemistry, vol. 3, Pergamon, Oxford, 1982, p. 1.
[6] W.N. Lipscomb, Boron Hydrides, Benjamin, New York, 1963.
[7] W.L. Jorgensen, L. Salem, The Organic Chemist's Book of Orbitals, Academic Press, New York, 1973.
[8] T.J. Coffy, G. Medford, J. Plotkin, G.J. Long, J.C. Huffman, S.G. Shore, Organometallics 8 (1989) 2404.
[9] R.L. DeKock, P. Deshmukh, T.P. Fehlner, C.E. Housecroft, J.S. Plotkin, S.G. Shore, J. Am. Chem. Soc. 105 (1983) 815.
[10] C.R. Brundle, M.B. Robin, H. Basch, M. Pinsky, A. Bond, J. Am. Chem. Soc. 92 (1970) 3863.
[11] A. Moezzi, M.M. Olmstead, P.P. Power, J. Am. Chem. Soc. 114 (1992) 2715.
[12] T.B. Marder, N.C. Norman, C.R. Rice, E.G. Robins, Chem. Commun. (1997) 53.
[13] M.R. Smith III, Prog. Inorg. Chem. 48 (1999) 505.
[14] E.K. Pham, R. West, J. Am. Chem. Soc. 111 (1989) 7667.
[15] D.H. Berry, J.H. Chey, H.S. Zipin, P.J. Carroll, J. Am. Chem. Soc. 112 (1990) 452.
[16] S.A. Cohen, P.R. Auburn, J.E. Bercaw, J. Am. Chem. Soc. 105 (1983) 1136.
[17] T.R. Cundari, M.S. Gordon, J. Mol. Theor. Chem. 119 (1994) 47.
[18] S. Sakaki, M. Ieki, Inorg. Chem. 30 (1991) 4218.
[19] J.A. Ulman, E.L. Andersen, T.P. Fehlner, J. Am. Chem. Soc. 100 (1978) 456.
[20] A.H. Cowley, N.C. Norman, Prog. Inorg. Chem. 34 (1986) 1.
[21] A.H. Cowley, Polyhedron 3 (1984) 389.
[22] J. Borm, L. Zsolnai, G. Huttner, Angew. Chem. Int. Ed. Engl. 22 (1983) 977.

[23] K.A. Schugard, R.F. Fenske, J. Am. Chem. Soc. 107 (1985) 3384.
[24] A.L. Rizopoulos, M.P. Sigalas, New J. Chem. 18 (1994) 197.
[25] I. Ando, G.B. Webb, Theory of NMR Parameters, Academic Press, New York, 1983.
[26] C.E. Housecroft, T.P. Fehlner, Adv. Organomet. Chem. 21 (1982) 57.
[27] J.D. Kennedy, Prog. Inorg. Chem. 32 (1984) 519.
[28] J.D. Kennedy, Prog. Inorg. Chem. 34 (1986) 211.
[29] R.N. Grimes, Acc. Chem. Res. 11 (1978) 420.
[30] R.N. Grimes, in: R.N. Grimes (Ed.), Metal Interactions with Boron Clusters, Plenum, New York, 1982 (269 pp.).
[31] L.J. Guggenberger, A.R. Kane, E.L. Muetterties, J. Am. Chem. Soc. 94 (1972) 5665.
[32] N.N. Greenwood, J.D. Kennedy, D. Reed, J. Chem. Soc. Dalton Trans. (1980) 196.
[33] J. Bould, N.N. Greenwood, J.D. Kennedy, W.S. McDonald, J. Chem. Soc. Dalton Trans. (1985) 1843.
[34] C.E. Housecroft, B.A.M. Shaykh, A.L. Rheingold, B.S. Haggerty, Inorg. Chem. 30 (1991) 125.
[35] C.E. Housecroft, S.M. Owen, P.R. Raithby, B.A.M. Shaykh, Organometallics 9 (1990) 1617.
[36] J. Bould, J.D. Kennedy, W.S. Mcdonald, Inorg. Chim. Acta 196 (1992) 201.
[37] B.S. Haggerty, C.E. Housecroft, A.L. Rheingold, B.A.M. Shaykh, J. Chem. Soc. Dalton Trans. (1991) 2175.
[38] X. Lei, M. Shang, T.P. Fehlner, Organometallics 17 (1998) 1558.
[39] X. Lei, M. Shang, T.P. Fehlner, J. Am. Chem. Soc. 121 (1999) 1275.
[40] X. Lei, A.K. Bandyopadhyay, M. Shang, T.P. Fehlner, Organometallics 18 (1999) 2294.
[41] D.F. Gaines, S.J. Hildebrandt, Inorg. Chem. 17 (1978) 794.
[42] S.J. Hildebrandt, D.F. Gaines, J.C. Calabrese, Inorg. Chem. 17 (1978) 790.
[43] C.E. Housecroft, T.P. Fehlner, Inorg. Chem. 21 (1982) 1739.
[44] S.K. Boocock, M.A. Toft, K.E. Inkrott, L.-Y. Hsu, J.C. Huffman, K. Folting, S.G. Shore, Inorg. Chem. 23 (1984) 3084.
[45] X. Lei, M. Shang, T.P. Fehlner, Chem. — Eur. J. 6 (2000) 2653.
[46] R. Weiss, J.R. Bowser, R.N. Grimes, Inorg. Chem. 17 (1978) 1522.
[47] T.L. Venable, R.N. Grimes, Inorg. Chem. 21 (1982) 887.
[48] T.L. Venable, E. Sinn, R.N. Grimes, J. Chem. Soc. Dalton Trans. (1984) 2275.
[49] Y. Nishihara, K.J. Deck, M. Shang, T.P. Fehlner, B.S. Haggerty, A.L. Rheingold, Organometallics 13 (1994) 4510.
[50] R. Weiss, R.N. Grimes, Inorg. Chem. 18 (1979) 3291.
[51] C.N. Iverson, M.R. Smith III, J. Am. Chem. Soc. 121 (1999) 7696.
[52] H. Chen, S. Schlecht, T.C. Semple, J.F. Hartwig, Science 287 (2000) 1995.